



**SAPIENZA**  
UNIVERSITÀ DI ROMA

EARTH OBSERVATION DATA ANALYSIS

---

## Surface Mapping from MSI Sentinel-2 Data

---

Ivan Colantoni

1704031

colantoni.1704031@studenti.uniroma1.it

Federico Parente

1716030

parente.1716030@studenti.uniroma1.it

## Contents

<b>1</b>	<b>Introduction</b>	<b>2</b>
1.1	Data Exploration . . . . .	2
1.2	Classification Mask . . . . .	3
1.3	Subset around Lake Bracciano . . . . .	3
<b>2</b>	<b>Normalized Index</b>	<b>4</b>
2.1	Water . . . . .	4
2.2	Vegetation . . . . .	5
<b>3</b>	<b>Sea Chlorophyll-a and Sediment Estimation</b>	<b>6</b>
3.1	Subsetting around Ostia-Fiumicino . . . . .	6
3.2	EmpReg Algorithm . . . . .	6
3.3	Comparison . . . . .	7
3.4	MCI algorithm . . . . .	8
<b>4</b>	<b>Scene Classification</b>	<b>8</b>
4.1	Vector creation . . . . .	8
4.2	Supervised Classification algorithm . . . . .	9
<b>References</b>		<b>10</b>

## 1 Introduction

**Objective:** Explore Sentinel-2 MSI data for estimating vegetation cover, inland water, chlorophyll-a sea concentration and supervised classification within a region of interested (ROI). We have downloaded the MSI imagery provided by ESA-RSS in the VM folder, giving the details in fig. 1 and 2

Figure 1: Product Details Winter Image

PRODUCT_START_TIME	2017-12-22T10:04:19.027Z
PRODUCT_STOP_TIME	2017-12-22T10:04:19.027Z
PRODUCT_URI_1C	S2B_MSIL1C_20171222T100419_N0206_R122_T32TQM_20171222T120817.SAFE
PRODUCT_URI_2A	S2B_MSIL2A_20171222T100419_N0206_R122_T32TQM_20171222T120817.SAFE
PROCESSING_LEVEL	Level-2Ap
PRODUCT_TYPE	S2MSI2Ap
PROCESSING_BASELINE	02.06

Figure 2: Product Details Summer Image

PRODUCT_START_TIME	2017-08-29T10:00:31.026Z
PRODUCT_STOP_TIME	2017-08-29T10:00:31.026Z
PRODUCT_URI_1C	S2A_MSIL1C_20170829T100031_N0205_R122_T32TQM_20170829T100026.SAFE
PRODUCT_URI_2A	S2A_MSIL2A_20170829T100031_N0205_R122_T32TQM_20170829T100026.SAFE
PROCESSING_LEVEL	Level-2Ap
PRODUCT_TYPE	S2MSI2Ap
PROCESSING_BASELINE	02.05

### 1.1 Data Exploration

The first step is to visualize the product through the RGB channels, in this case:

- 1 Red-channel = B4 (665nm)
- 2 Green-channel = B3 (560nm)
- 3 Blue-channel = B2(490nm)

and resulting in the images of figure 3



Figure 3: RGB Summer - Winter

## 1.2 Classification Mask

We built an RGB classification mask using the L2 MSI products. We assigned to each channel of the RGB image the *scl masks* defined in the products, respectively: *scl not vegetated*, *scl vegetated*, *scl water*. This led us to results showed in fig. 4. Note that the *not vegetated* part is much more visible in the summer product than the winter one, because of the massive presence of bare soil. Moreover the 'black' pixels represent what is not taken into account by the classification, in this case mostly clouds and urban areas.

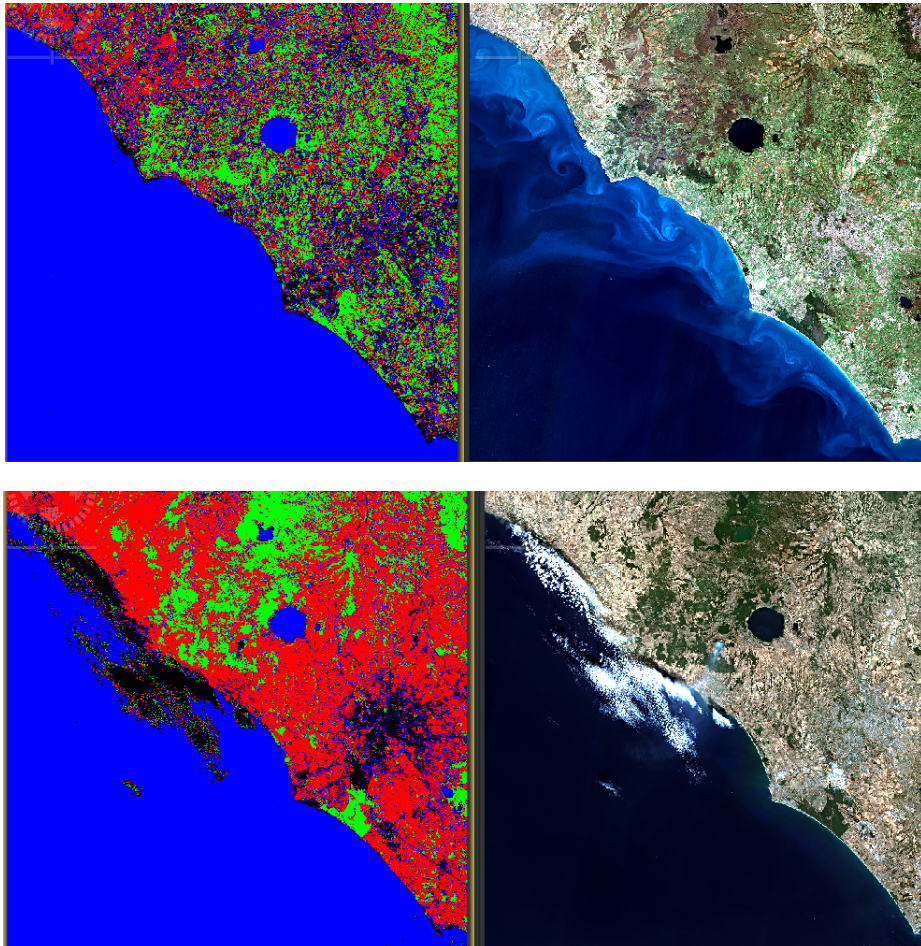


Figure 4: Classification mask for Winter (up) and Summer (down)

## 1.3 Subset around Lake Bracciano



Figure 5: Lake Bracciano summer - winter

Using the graph builder tool we subset the products around Lake Bracciano and resampled the B2, B3, B4 bands at 10 m. See fig. 5

## 2 Normalized Index

### 2.1 Water

We used the **Normalized Difference Water Index** algorithm implemented on snap. The NDWI is sensitive to changes in liquid water content of vegetation canopies. It is less sensitive to atmospheric effects than NDVI. The NDWI comes from the equation 1:

$$NDWI = \frac{IRfactor \times NIR - MIRfactor \times MIR}{IRfactor \times NIR + MIRfactor \times MIR} \quad (1)$$

We compared it to the **NDWI2**. The NDWI2 was developed to detect surface waters in wetland environments and to allow the measure of surface water extent. It results from the equation 2:

$$NDWI2 = \frac{Greenfactor \times Green - IRfactor \times NIR}{Greenfactor \times Green + IRfactor \times NIR} \quad (2)$$

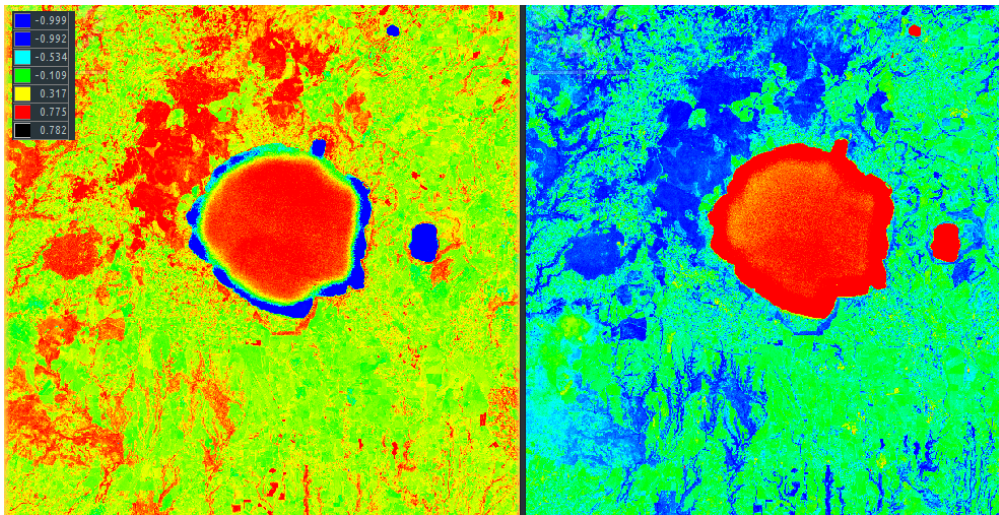


Figure 6: NDWI (left) and NDWI2 (right) index for Summer

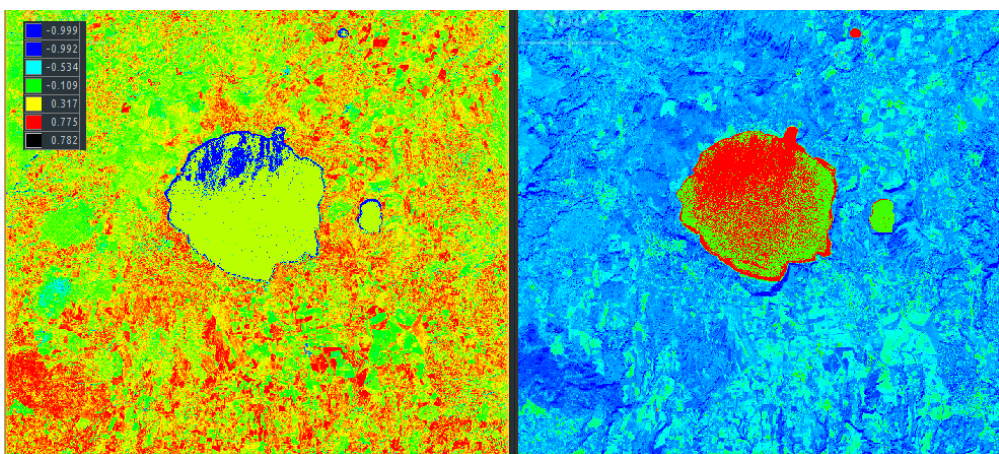
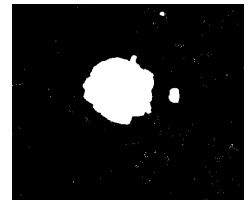


Figure 7: NDWI (left) and NDWI2 (right) index for Winter

Results are showed in fig. 7 and 6, and put in evidence that NDWI can be used to detect the water content in the leaves of crop areas while NDWI2 detect perfectly the bounds of the lake and other water areas. So NDWI2 can be used to build a water mask, like showed in the figure on the right.



## 2.2 Vegetation

We used the well-known **NDVI** index implemented on snap for both summer and winter products [4][5]. See fig. 8

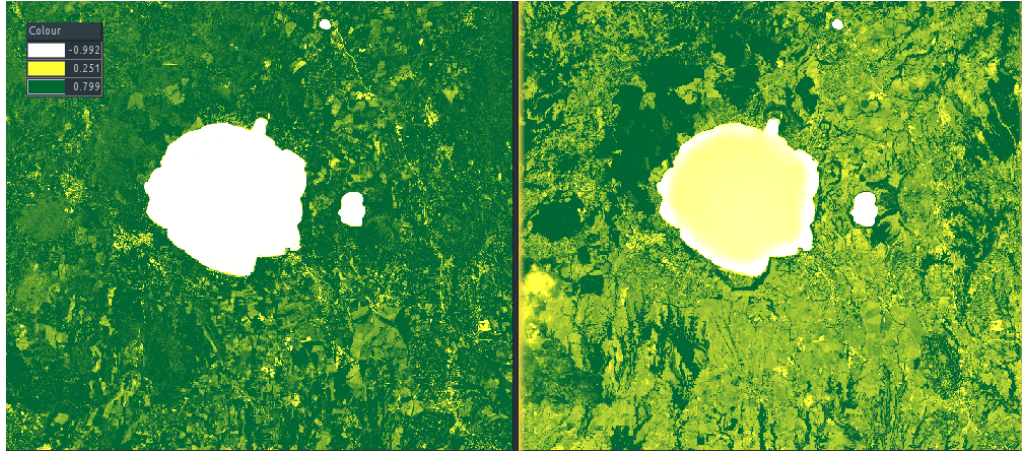


Figure 8: NDVI of winter (left) and summer (right)

We provide the histograms for the index related to summer (fig. 9) and winter (fig.10).

We see that for summer product the frequency of pixels with values above 0.4 is larger than the winter one (see blue area from 0.4 to 1.0 NDVI value), with peak on 0.5. This means that, in this case, the area has a more dense vegetation in the summer season. While for the winter product the maximum in the histogram is nearby -1.0, which means that there is a good concentration of water extent in the area.

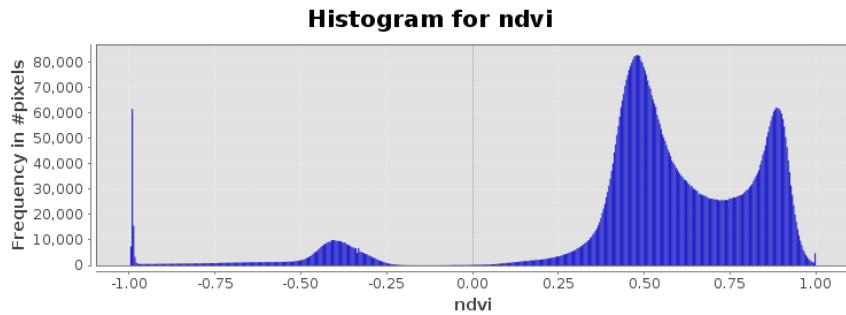


Figure 9: Summer

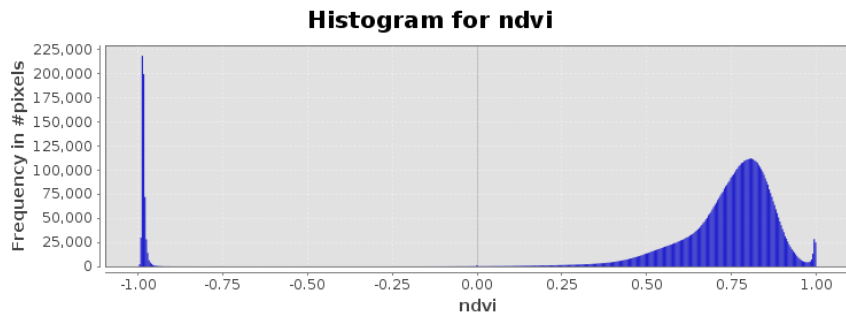


Figure 10: Winter

### 3 Sea Chlorophyll-a and Sediment Estimation

#### 3.1 Subsetting around Ostia-Fiumicino

We subset the images around the area of Ostia-Fiumicino, focusing on delta of Tiber river. See fig. 11



Figure 11: delta of Tiber, winter (left) summer (right)

#### 3.2 EmpReg Algorithm

Following [2] [3] we implemented the empirical regressive algorithm to estimate Chlorophyl-a (Chl-a) and Total suspended sediment (TSS). The first step is to build the Maximum Band Ratio (MBR) index, from the equation 3:

$$r_{MBR} = \frac{\max(R_{wlB1}, R_{wlB2})}{R_{wlB3}} \quad (3)$$

This index is used in eq. 4, given from the empirical regressive algorithm, to build the Chl-a.

$$C_{Chla} = a_1 \exp(-a_2 r_{MBR}) \quad (4)$$

For TSS we have eq. 5:

$$C_{TSM} = b_1 \exp(b_2 R_{wlB4}) \quad (5)$$

Using the *Band Maths* tool of snap, we created new bands, called Chl-a and TSS, implementing the expression of the equation 4 and 5. See fig. 12

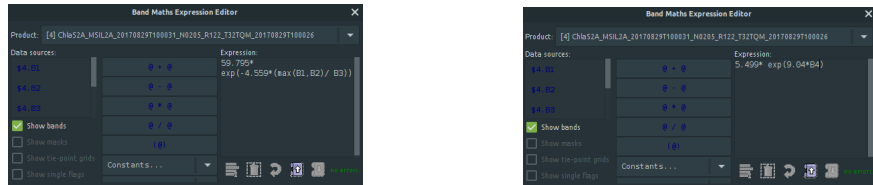


Figure 12: Implementations

We show the resulting images using the same color palette. See fig. 13 for Chl-a estimation and fig. 14 for TSS.

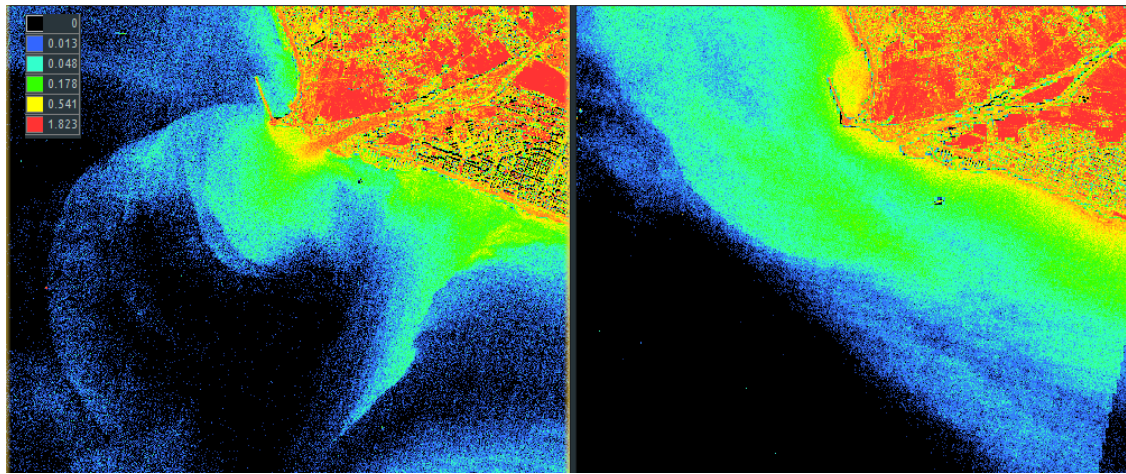


Figure 13: Chl-a estimation winter (left) summer (right)

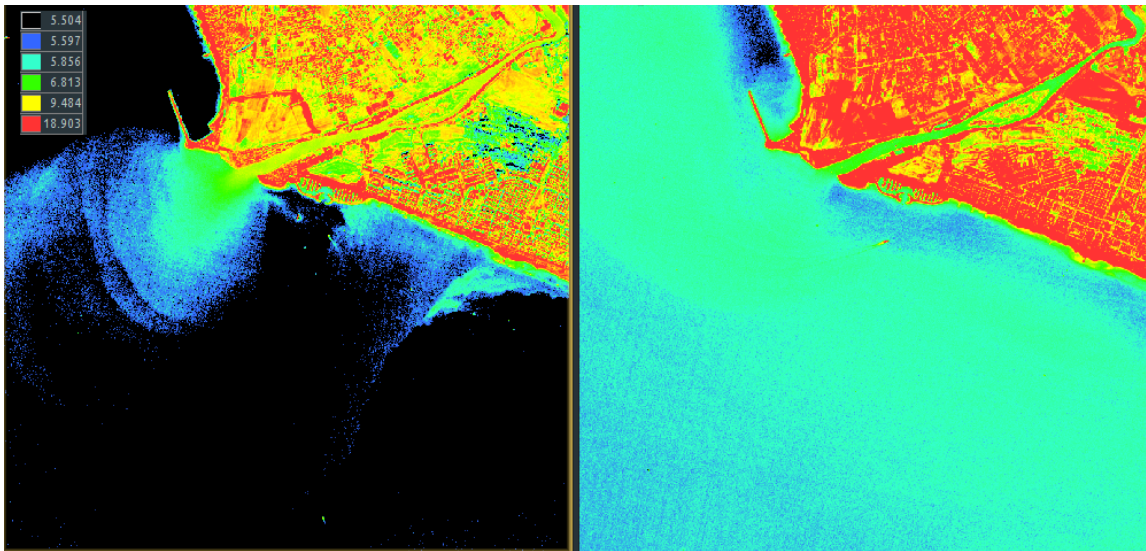


Figure 14: TSS estimation winter (left) summer (right)

### 3.3 Comparison

We performed a comparison between the estimated Chl-a and TSS by making the difference of images between winter and summer season. Results are reported in fig. ??

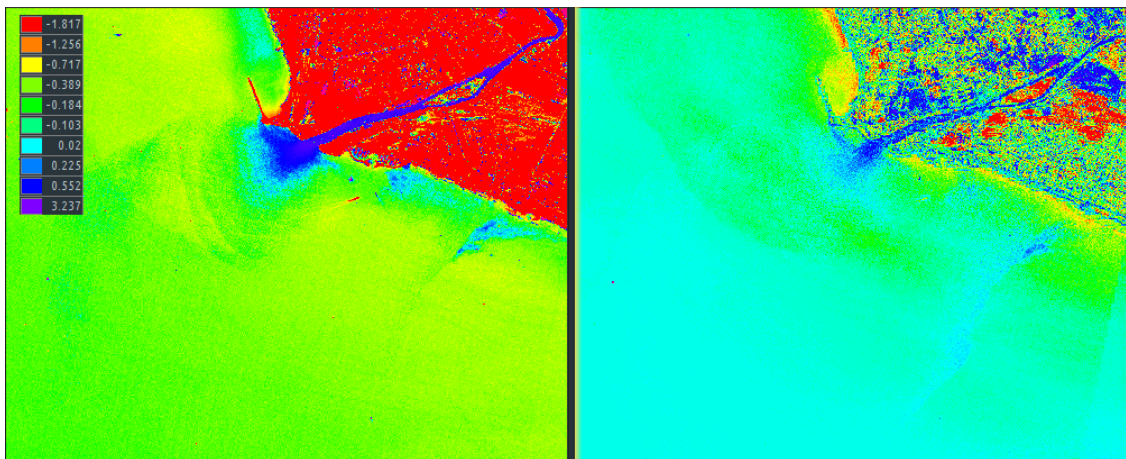


Figure 15: Image difference for TSS (left) and Chla (right)

### 3.4 MCI algorithm

We report the comparison between the obtained Chl-a estimation with the empirical regressive algorithm and the one performed using the MCI (Maximum Chlorophyll Index) algorithm implemented on snap. After having resampled the image at the resolution of 10m per pixel and selected the preset for MSI L2 product, we obtained the results showed in figure 16. Note that higher values are concentrated over the delta of the river, which is a meaningful result.

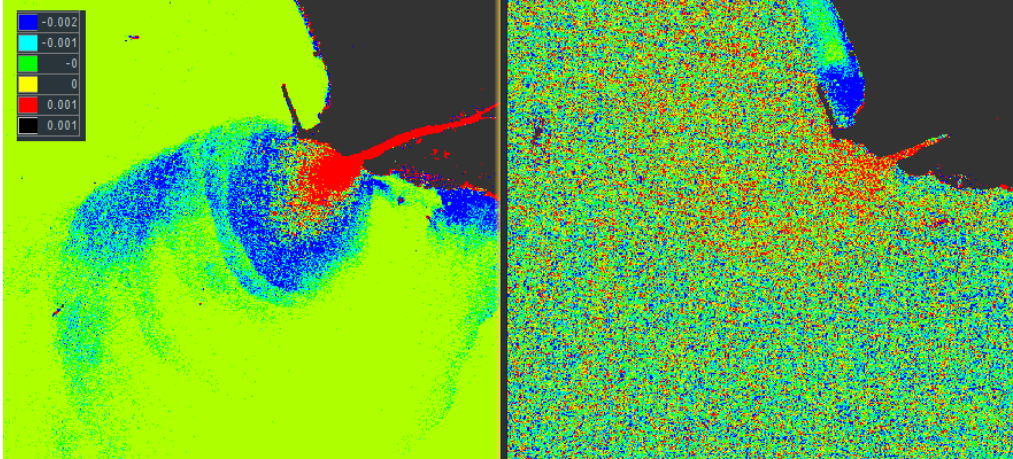


Figure 16: Maximum Chlorophyll Index for winter (left) and summer (right)

## 4 Scene Classification

### 4.1 Vector creation

Classifications aim to find a certain number of classes (4,5,10) and associate each pixel to a certain class [1]. In snap there are implemented different classification methods, both unsupervised and supervised. Before starting the supervised classification, the algorithm needs specify the vector the algorithm will use as training areas Fig.17.



Figure 17: vectors

## 4.2 Supervised Classification algorithm

The maximum likelihood classifier is a supervised classifier that will use the polygons in the figure to learn to classify the picture pixels in four categories: vegetation, water, urban areas and bare soil. See fig. 18.

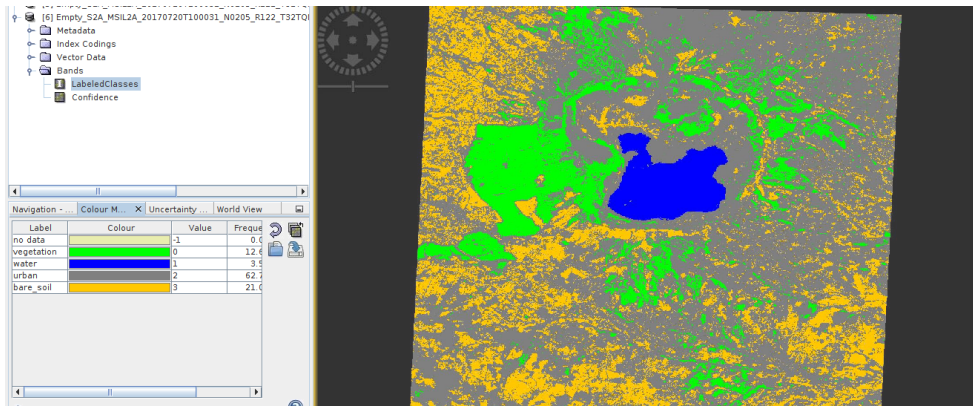


Figure 18: Maximum Likelihood classification

We compare that to the K-means clustering algorithm, set over 4 bands (B1, B2, B3, B4) and ran over 30 iterations. Results are showed here on fig. 19. It is clear that the unsupervised classification outperformed the supervised one.

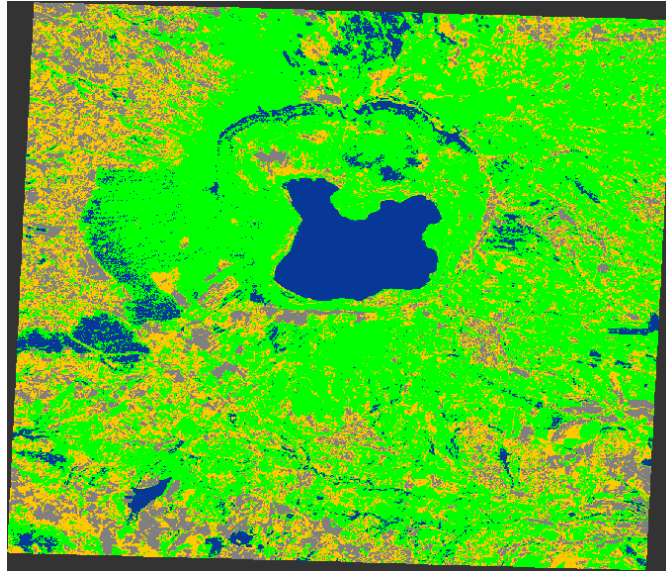


Figure 19: K-means clustering

## References

- [1] P. Defourny, G. Kirches, C. Brockmann, M. Boettcher, M. Peters, S. Bontemps, C. Lamarche, M. Schlerf, and M. Santoro. Land cover cci. *Product User Guide Version*, 2, 2012.
- [2] J.-B. Feret, C. François, G. P. Asner, A. A. Gitelson, R. E. Martin, L. P. Bidel, S. L. Ustin, G. le Maire, and S. Jacquemoud. Prospect-4 and 5: Advances in the leaf optical properties model separating photosynthetic pigments. *Remote Sensing of Environment*, 112(6):3030 – 3043, 2008.
- [3] M. Iacobolli, M. Orlandi, D. Cimini, and F. S. Marzano. Remote sensing of coastal water-quality parameters from sentinel-2 satellite data in the tyrrhenian and adriatic seas. In *2019 PhotonIcs & Electromagnetics Research Symposium-Spring (PIERS-Spring)*, pages 2783–2788. IEEE, 2019.
- [4] R. B. Myneni, F. G. Hall, P. J. Sellers, and A. L. Marshak. The interpretation of spectral vegetation indexes. *IEEE Transactions on Geoscience and Remote Sensing*, 33(2):481–486, 1995.
- [5] A. Viña, A. A. Gitelson, A. L. Ngay-Robertson, and Y. Peng. Comparison of different vegetation indices for the remote assessment of green leaf area index of crops. *Remote Sensing of Environment*, 115(12):3468–3478, 2011.